

Post-peak behavior and flexural ductility of doubly reinforced normal- and high-strength concrete beams

H.J. Pam[†], A.K.H. Kwan[‡] and J.C.M. Ho^{‡†}

Department of Civil Engineering, The University of Hong Kong, Pokfulam Road, Hong Kong

Abstract. The complete moment-curvature curves of doubly reinforced concrete beams made of normal- or high-strength concrete have been evaluated using a newly developed analytical method that takes into account the stress-path dependence of the constitutive properties of the materials. From the moment-curvature curves and the strain distribution results obtained, the post-peak behavior and flexural ductility of doubly reinforced normal- and high-strength concrete beam sections are studied. It is found that the major factors affecting the flexural ductility of reinforced concrete beam sections are the tension steel ratio, compression steel ratio and concrete grade. Generally, the flexural ductility decreases as the amount of tension reinforcement increases, but increases as the amount of compression reinforcement increases. However, the effect of the concrete grade on flexural ductility is fairly complicated, as will be explained in the paper. Quantitative analysis of such effects has been carried out and a formula for direct evaluation of the flexural ductility of doubly reinforced concrete sections developed. The formula should be useful for the ductility design of doubly reinforced normal- and high-strength concrete beams.

Keywords: flexural ductility; high-strength concrete; moment-curvature behavior; reinforced concrete beams.

1. Introduction

In the design of a reinforced concrete beam, both the flexural strength and ductility need to be considered. However, whilst the flexural strength can be quite easily evaluated by the ordinary beam bending theory, the flexural ductility cannot be determined directly by any simple method (Park and Paulay 1975). Because of the difficulties involved, ductility analysis is seldom carried out in normal design practice. But this does not imply that the flexural ductility of a beam is unimportant. From the structural safety point of view, ductility is at least as important as strength. Good flexural ductility provides the beam a much better chance of survival when it is overloaded or subjected to strong impact.

If normal-strength concrete is used for the beam, the flexural ductility is, in most cases, not critical and it is usually sufficient to just limit the tension steel ratio so that the beam is under-reinforced. However, if high-strength concrete, which is generally more brittle, is used, more careful checking of the flexural ductility is considered advisable. A recent experimental study by Pam *et al* (2001) has indicated that a reinforced high-strength concrete beam, if not properly designed, could

[†] Associate Professor
[‡] Senior Lecturer
^{‡†} Graduate Student

fail in a rather brittle manner and that just limiting the tension steel ratio to keep the beam under-reinforced might not be sufficient to maintain the flexural ductility of a high-strength concrete beam at the same minimum level as that normally provided in a normal-strength concrete beam. Nevertheless, because of obvious advantages, the use of high-strength concrete is increasing (ACI Committee 363 1992). To ensure that high-strength concrete beams are provided with sufficient ductility, detailed investigation of the effect of concrete grade on flexural ductility is urgently needed.

Irrespective of whether normal- or high-strength concrete is used, the flexural ductility can become critical when the concrete section is relatively small and a relatively large amount of tension reinforcement has to be added to achieve the required flexural strength. This problem may be resolved by increasing the beam size or by adding compression reinforcement. However, a larger size beam will increase dead weight and may impose difficulties on the design of the geometric layout. The addition of compression reinforcement is a good way to restore the flexural ductility to a higher level, but this will lead to a significantly higher cost, which may or may not be justified depending on the situation and the resulting increase in flexural ductility. To understand better the possible increase in flexural ductility due to the addition of compression reinforcement, detailed ductility analysis of beam sections with or without compression reinforcement added is required.

However, there is no simple method for direct evaluation of flexural ductility. To evaluate the flexural ductility of a beam section, it is necessary to first analyze the complete moment-curvature relation of the section covering both the pre-peak and post-peak ranges and then calculate the amount of inelastic curvature that the section can sustain before failure. Whatever method employed, a nonlinear structural analysis, using the actual stress-strain curves of the constitutive materials and an iterative numerical procedure, is required. Up to now, very limited analysis of the complete moment-curvature relation of reinforced concrete sections has been carried out (Carreira and Chu 1986, Samra *et al.* 1996, Sheikh and Yeh 1997) and as a result there has been few data on the flexural ductility of reinforced concrete beams.

The authors have recently developed a new method of analyzing the complete moment-curvature behavior of reinforced concrete beam sections that not only uses the actual stress-strain curves but also takes into account the stress-path dependence of the constitutive properties of the materials (Ho *et al.* 2001). Application of the method to analyze the post-peak behavior of reinforced concrete beam sections has revealed that at the post-peak stage, the neutral axis depth keeps on increasing and beyond a certain point, the strain in the tension reinforcement starts to decrease. To cater for such strain reversal, the stress-path dependence of the stress-strain relation of the steel reinforcement must be taken into account. In fact, the numerical results have indicated that the negligence of the stress-path dependence of the material properties in the previous analysis methods developed by others could lead to significant errors in the post-peak moment-curvature relation and flexural ductility.

The analysis method developed by the authors has so far been applied only to singly reinforced sections. However, doubly reinforced sections with both tension and compression reinforcement provided are equally important because very often a high-strength concrete beam is provided with a relatively large amount of tension reinforcement thereby rendering the flexural ductility of the beam very critical and leading to no other alternative apart from adding compression reinforcement. In the present study, this newly developed method is applied to analyze the post-peak moment-curvature behavior and flexural ductility of doubly reinforced normal- and high-strength concrete beam sections.

2. Stress-strain curve of concrete

To compare the flexural behaviors of normal- and high-strength concrete beams, a complete stress-strain curve model that is applicable to both normal- and high-strength concretes is needed. Herein, the stress-strain curve model developed by Attard and Setunge (1996), which has been shown to be applicable to a broad range of concrete strength from 20 to 130 MPa, is used. The main parameters employed to establish the equation were the initial Young’s modulus E_c , peak stress f_{co} , strain at peak ϵ_{co} , and the stress f_{ci} and strain ϵ_{ci} at the inflection point on the descending branch of the stress-strain curve. It is given by:

$$\sigma_c/f_{co} = \frac{A(\epsilon_c/\epsilon_{co}) + B(\epsilon_c/\epsilon_{co})^2}{1 + (A - 2)(\epsilon_c/\epsilon_{co}) + (B + 1)(\epsilon_c/\epsilon_{co})^2} \quad (1)$$

in which σ_c and ϵ_c are respectively the stress and strain in the concrete. To allow for the difference between the in-situ uniaxial compressive strength and the cylinder strength, the peak stress f_{co} may be taken as 0.9 times the cylinder strength f_c . The parameters A and B have been obtained by Attard and Stewart (1998) as follows:

For ascending branch of the stress-strain curve,

$$A = \frac{E_c \epsilon_{co}}{f_{co}} \quad (2a)$$

$$B = \frac{(A - 1)^2}{0.55} - 1 \quad (2b)$$

For descending branch of the stress-strain curve,

$$A = \frac{f_{ci}(\epsilon_{ci} - \epsilon_{co})^2}{\epsilon_{co} \epsilon_{ci} (f_{co} - f_{ci})} \quad (3a)$$

$$B = 0 \quad (3b)$$

In the above, the values of E_c , ϵ_{co} , f_{ci} and ϵ_{ci} may be determined from:

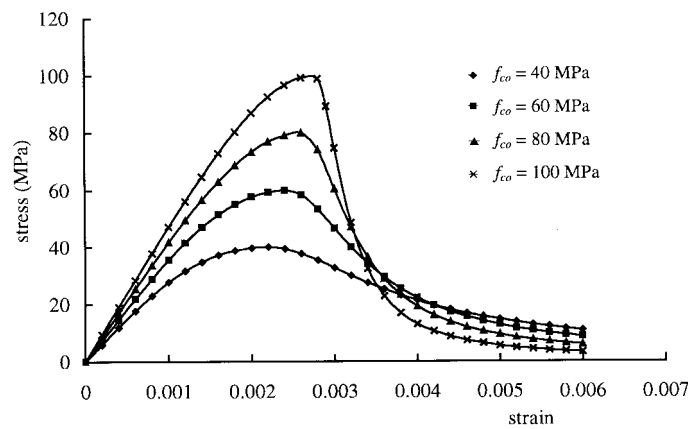


Fig. 1 Stress-strain curves of concrete derived from Attard and Setunge’s model

$$E_c = 4370 (f_{co})^{0.52} \quad (4a)$$

$$\varepsilon_{co} = 4.11 (f_{co})^{0.75}/E_c \quad (4b)$$

$$f_{ci}/f_{co} = 1.41 - 0.17 \ln(f_{co}) \quad (4c)$$

$$\varepsilon_{ci}/\varepsilon_{co} = 2.50 - 0.30 \ln(f_{co}) \quad (4d)$$

where E_c and f_{co} are in MPa and ε_{co} is dimensionless. Fig. 1 shows some typical stress-strain curves derived from Attard and Setunge's model.

3. Stress-strain curve of steel reinforcement

The steel reinforcement is assumed to be linear elastic-perfectly plastic. To cater for strain reversal, the stress-path dependence of the stress-strain relation is taken into account by assuming that the unloading path follows the initial elastic slope, as shown in Fig. 2. Incorporating stress-path dependence, the stress-strain equation of the steel reinforcement may be formulated as follows. When the strain is increasing, the stress in the steel is given by:

$$\text{at elastic stage:} \quad \sigma_s = E_s \varepsilon_s \quad (5a)$$

$$\text{after yielding:} \quad \sigma_s = f_y \quad (5b)$$

in which σ_s and ε_s are respectively the stress and strain in the steel, E_s is the Young's modulus and f_y is the yield stress. At the initial elastic stage, there is no residual plastic strain but after yielding, there will be a residual plastic strain ε_p given by:

$$\varepsilon_p = \varepsilon_s - \sigma_s/E_s \quad (6)$$

On the other hand, when the strain is decreasing, the stress in the steel becomes:

$$\sigma_s = E_s (\varepsilon_s - \varepsilon_p) \quad (7)$$

where ε_p is the residual strain at the end of the last strain increasing cycle.

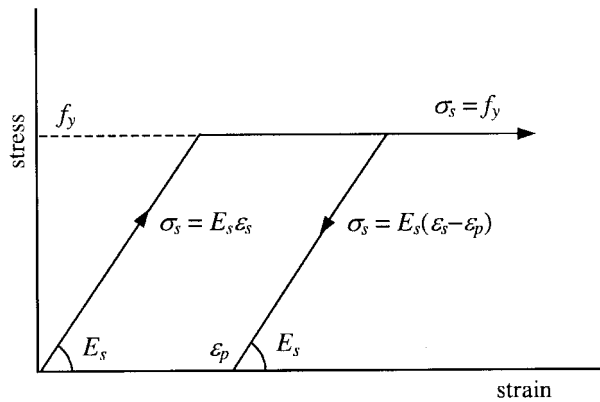


Fig. 2 Stress-strain curve of steel with stress-path dependence allowed for

4. Nonlinear bending theory for reinforced concrete beams

Three basic assumptions are made in the derivation of the theory: (1) plane sections before bending remain plane after bending; (2) the tensile strength of the concrete may be neglected; and (3) there is no bond-slip between the reinforcement bars and the concrete. They are all commonly accepted and are nearly exact except in deep beams or in localized areas near cracks.

For convenience, the sign conventions adopted are such that all strain and stress quantities are positive: (1) compressive strain and stress in concrete are positive; (2) compressive strain and stress in compression reinforcement are positive; and (3) tensile strain and stress in tension reinforcement are positive.

Referring to Fig. 3 and denoting the curvature of the beam by ϕ , the strain developed in the beam section is given by:

$$\varepsilon = \phi x \tag{8}$$

where x is the distance from the neutral axis. Having determined the strains, the corresponding stresses developed in the concrete and steel reinforcement may be evaluated from their respective stress-strain curves. The stresses developed in the beam section must satisfy the conditions of axial equilibrium and moment equilibrium. Axial equilibrium leads to:

$$P = \int_0^{d_n} \sigma_c b dx + \sum A_{sc} \sigma_{sc} - \sum A_{st} \sigma_{st} \tag{9}$$

in which P is the applied axial load (compression force positive). On the other hand, moment equilibrium leads to:

$$P = \int_0^{d_n} \sigma_c b x dx + \sum A_{sc} \sigma_{sc} (d_n - d_1) + \sum A_{st} \sigma_{st} (d - d_n) \tag{10}$$

in which M is the resisting moment (sagging moment positive). If no axial load is applied, a value of zero is assigned to P .

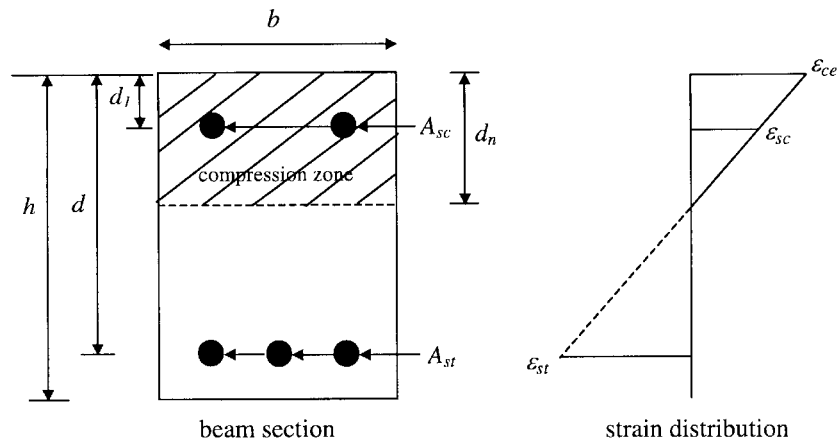


Fig. 3 A beam section subjected to bending moment

5. Method of analysis

The moment-curvature relation of the beam section is analyzed by applying prescribed curvature to the beam section incrementally in very small steps starting from zero curvature. For a given curvature, the strains developed in the section are first evaluated based on an assumed or the previous value of the neutral axis depth. From the strains evaluated, the corresponding stresses developed in the concrete and the steel reinforcement are determined from their respective stress-strain curves.

Axial equilibrium of the beam section is then checked. Normally, the axial equilibrium condition is not immediately satisfied and there is an unbalanced axial force. An iterative procedure of successively adjusting the neutral axis depth until the unbalanced axial force is negligibly small is used to satisfy the axial equilibrium condition. Having determined the neutral axis depth that would satisfy the axial equilibrium condition, the resisting moment of the beam section is evaluated from the moment equilibrium condition. This gives a pair of curvature and moment values.

The above numerical process is repeated for each prescribed curvature value and continued until the curvature is large enough for the resisting moment to increase to the peak and decrease to less than 50% of the peak value.

6. Results of analysis

6.1 Sections analyzed

The beam sections analyzed are the same as the one shown in Fig. 3. These beam sections are given constant dimensions of $b = 300$ mm, $h = 600$ mm, $d = 550$ mm, and $d_l = 50$ mm. They represent typical doubly reinforced rectangular beam sections. For parametric study, the in-situ concrete compressive strength (peak stress in the stress-strain curve) f_{co} is varied from 30 to 100 MPa to cover both normal- and high-strength concretes, the compression steel ratio ρ_c ($\rho_c = A_{sc}/bd$) is varied from 0 to 2% to cover the case with no compression reinforcement added and the case with compression reinforcement added, and the tension steel ratio ρ_t ($\rho_t = A_{st}/bd$) is varied from 0.4 to 2.0 times the balanced steel ratio to cover both under-reinforced and over-reinforced sections. On the other hand, the steel reinforcement is assumed to have constant properties with $f_y = 460$ MPa and $E_s = 200$ GPa.

6.2 Complete moment-curvature relation and general behavior

Some selected moment-curvature curves of the beam sections analyzed are plotted in Fig. 4. It is seen that the moment-curvature curves of under- and over-reinforced sections have very different shapes. In the case of an under-reinforced section, the moment-curvature curve is almost linear before the peak moment is reached and there is a fairly long yield plateau at the post-peak stage before the resisting moment drops more rapidly till complete failure. However, in the case of an over-reinforced section, the moment-curvature curve is more like a single smooth curve with a sharp peak.

To study the nonlinear flexural behavior of the beam sections, the variations of the neutral axis depth d_n , the concrete strain at extreme compression fiber ϵ_{ce} , the steel strain in the tension

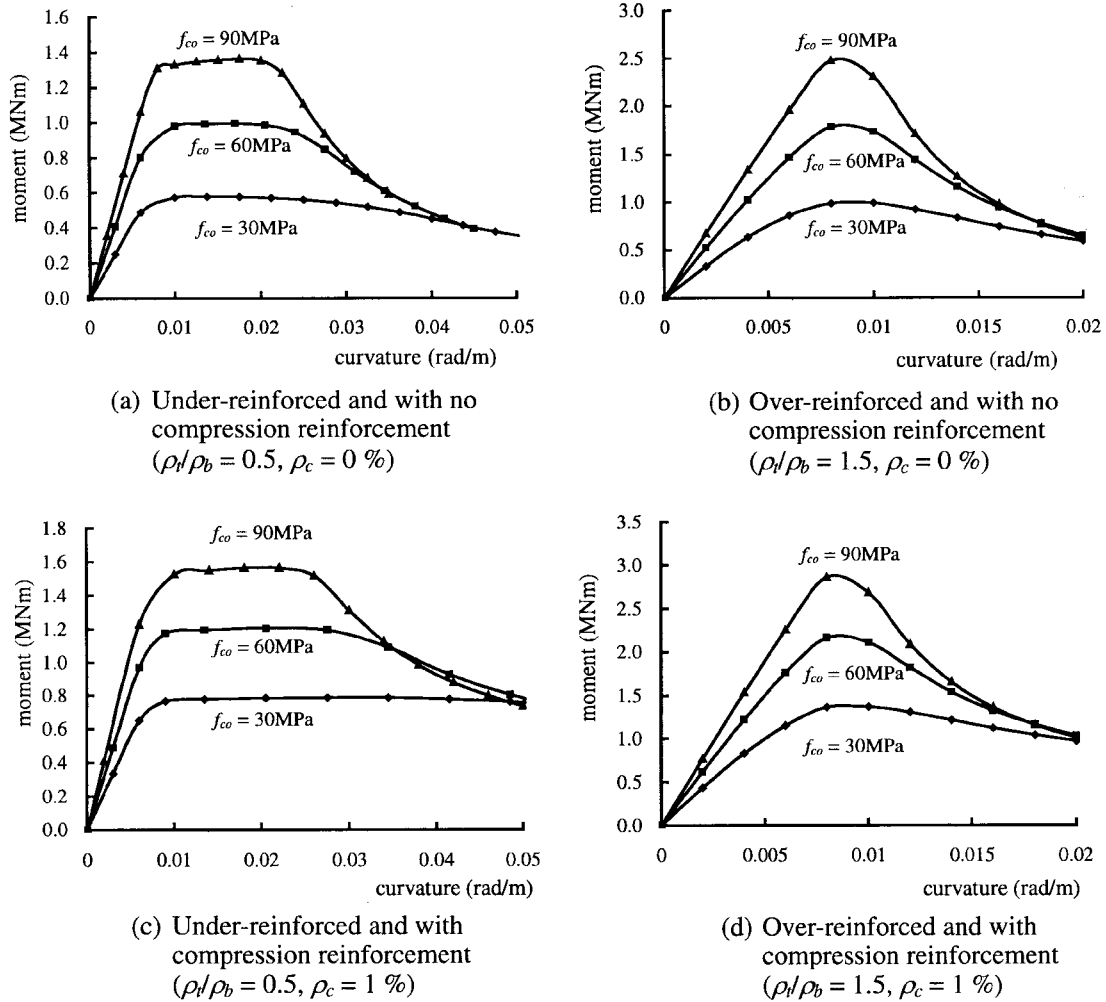


Fig. 4 Complete moment-curvature curves of some beam sections analyzed

reinforcement ϵ_{st} and the steel strain in the compression reinforcement ϵ_{sc} with the curvature ϕ in some typical sections are plotted in Fig. 5. It is seen that initially, the neutral axis depth remains almost constant. As the curvature increases and the concrete becomes inelastic, the neutral axis depth gradually decreases or increases depending on whether the section is under- or over-reinforced. However, regardless of whether the section is under- or over-reinforced, after entering into the post-peak stage, the neutral axis depth starts to increase rapidly and beyond a certain point, the strain in the tension reinforcement starts to decrease causing strain reversal. This strain reversal phenomenon in the tension reinforcement occurs in all sections. On the other hand, the strain in the compression reinforcement, if provided, always increases monotonically.

6.3 Failure mode and balanced steel ratio

In both sections with or without compression reinforcement provided, three failure modes have

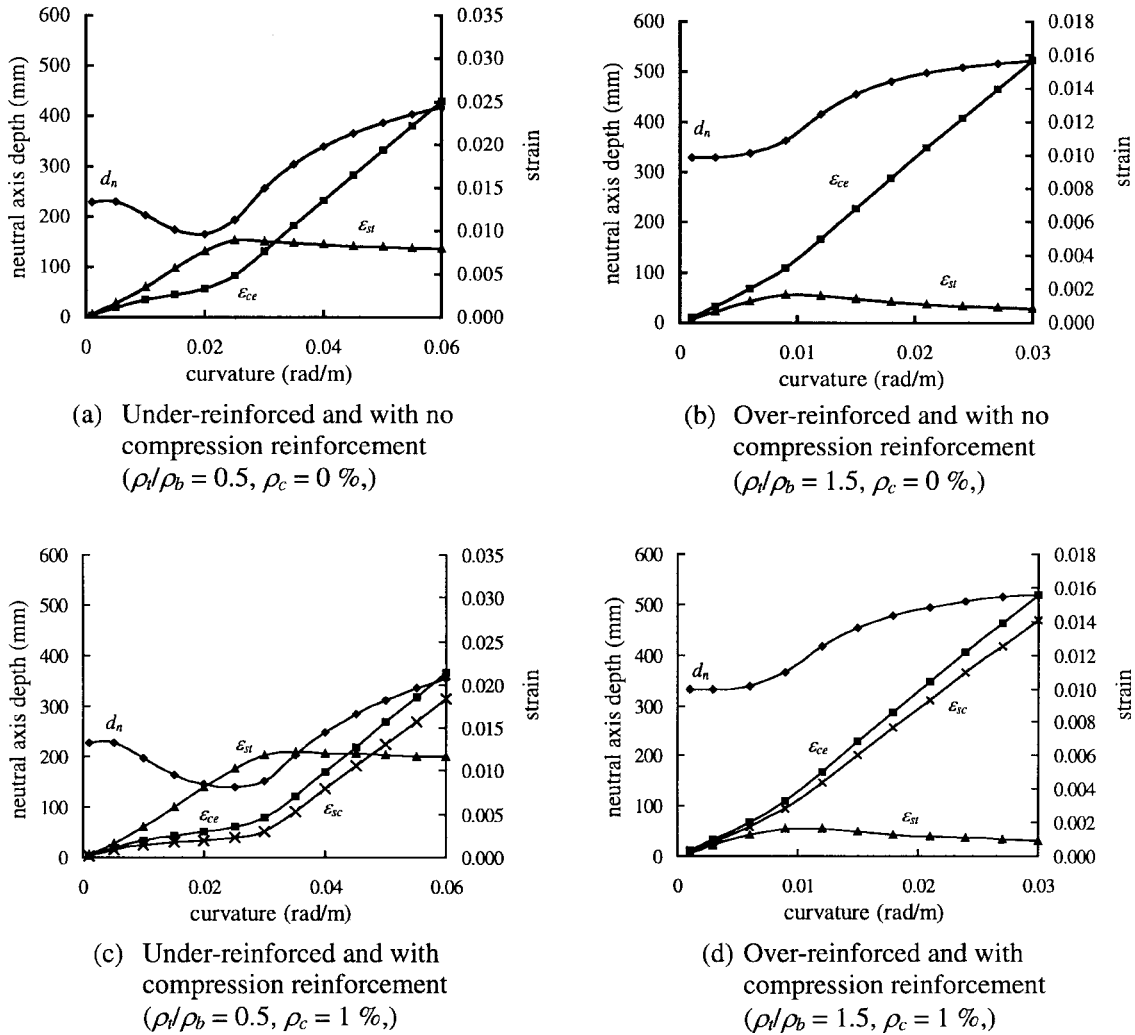


Fig. 5 Changes of neutral axis depth, concrete strain and steel strain with curvature for beam sections with $f_{co} = 60$ MPa

been observed: (1) tension failure under which the tension reinforcement yields before the concrete fails in compression; (2) compression failure under which the tension reinforcement remains unyielded even when the concrete has failed in compression completely; and (3) balanced failure under which the tension reinforcement just yields when the concrete fails in compression. For given concrete strength and compression steel ratio, there is a tension steel ratio that will lead to balanced failure. Such a tension steel ratio is called balanced steel ratio and is denoted hereafter by ρ_b . At a tension steel ratio smaller than the balanced steel ratio, tension failure will occur and at a tension steel ratio larger than the balanced steel ratio, compression failure will occur. Since the failure mode will affect the flexural ductility of the beam, it is important to determine the balanced steel ratio so that the failure mode may be predicted.

In this study, the balanced steel ratio is evaluated by a trial and error process of analyzing beam sections with different tension steel ratios and checking whether the tension reinforcement has ever

Table 1 Balanced steel ratios evaluated by nonlinear flexural analysis

f_{co} (MPa)	Balanced steel ratio ρ_b (%)				
	$\rho_c = 0\%$	$\rho_c = 0.5\%$	$\rho_c = 1.0\%$	$\rho_c = 1.5\%$	$\rho_c = 2.0\%$
30	3.19	3.69	4.19	4.69	5.19
40	3.95	4.45	4.95	5.45	5.95
50	4.69	5.19	5.69	6.19	6.69
60	5.39	5.89	6.39	6.89	7.39
70	6.06	6.56	7.06	7.56	8.06
80	6.70	7.20	7.70	8.20	8.70
90	7.30	7.80	8.30	8.80	9.30
100	7.87	8.37	8.87	9.37	9.87

yielded. It has been found during such analysis that at a relatively low tension steel ratio, the tension reinforcement yields right at the point of peak moment. However, at a relatively high tension steel ratio close to the balanced steel ratio, the tension reinforcement does not yield at the point of peak moment, but rather yields within the yield plateau range after the point of peak moment. So long that the tension reinforcement yields before the beam section fails completely, regardless of when it yields, the beam section is regarded as an under-reinforced section. If the tension reinforcement just yields before strain reversal as the beam section is loaded till complete failure, the beam section is regarded as a balanced section and its tension steel ratio taken as the balanced steel ratio. The balanced steel ratios so obtained are listed in Table 1.

It is seen that at a fixed concrete strength, the balanced steel ratio ρ_b increases linearly with the compression steel ratio ρ_c . In fact, the difference $(\rho_b - \rho_c)$ is found to be independent of ρ_c . Denoting this difference by ρ_{bo} , which is actually the balanced steel ratio of the section when no compression reinforcement is provided, the balanced steel ratio ρ_b may be obtained as:

$$\rho_b = \rho_{bo} + \rho_c \quad (11)$$

The value of ρ_{bo} is found to increase with the concrete strength but not in direct proportion because the percentage increase in balanced steel ratio is generally smaller than the percentage increase in concrete strength.

6.4 Ultimate concrete strain

The ultimate concrete strain ε_{cu} of a beam section is determined as the value of ε_{ce} when the beam section develops its peak resisting moment. Some of the ε_{cu} results for sections with $f_{co} = 60$ MPa, $\rho_c = 0, 1$ and 2% , and ρ_t varying from 0.4 to 2.0 times the balanced steel ratio are listed in Table 2. It is seen that for given concrete strength and compression steel ratio, the ultimate concrete strain remains more or less constant when the tension steel ratio is smaller than the balanced steel ratio. However, as the tension steel ratio increases to beyond the balanced steel ratio, the ultimate concrete strain increases quite abruptly to a certain maximum value. Then, as the tension steel ratio further increases, the ultimate concrete strain gradually decreases.

Although the variations of the ultimate concrete strain with the compression and tension steel ratios are quite complicated, the actual value of ultimate concrete strain used in the design has little effect on the calculated value of flexural strength. Therefore, it is better to adopt a single design value of ultimate concrete strain for a given concrete grade regardless of the steel ratios, provided

Table 2 Ultimate concrete strains (in $\mu\epsilon$) for beam sections with $f_{co} = 60$ MPa

ρ_t/ρ_b	$\rho_c = 0\%$			$\rho_c = 1\%$			$\rho_c = 2\%$		
	ϵ_{cu}	ϵ_{cu}'	ϵ_{cu}''	ϵ_{cu}	ϵ_{cu}'	ϵ_{cu}''	ϵ_{cu}	ϵ_{cu}'	ϵ_{cu}''
0.40	2775	2130	3450	2905	2225	4365	2970	2040	6140
0.60	2775	2270	3305	3010	2400	3605	3260	2475	3975
0.80	2775	2460	3230	2860	2500	3290	2900	2575	3380
1.00	3215	2955	3525	3230	2940	3565	3240	2925	3605
1.25	3185	2915	3480	3190	2905	3500	3195	2885	3535
1.50	3160	2895	3440	3160	2875	3455	3165	2860	3485
1.75	3135	2870	3405	3135	2855	3420	3130	2840	3445
2.00	3110	2855	3380	3105	2835	3395	3100	2820	3415
Max.	–	2955	–	–	2940	–	–	2925	–
Min.	–	–	3230	–	–	3290	–	–	3380

the error so introduced in the calculated value of flexural strength is acceptably small.

During the nonlinear analysis, it has been found that near the peak of the moment-curvature curve, the concrete strain at the extreme compression fiber ϵ_{ce} increases substantially while there is little change in the resisting moment. To study the range of variation of ϵ_{ce} near the peak of the moment-curvature curve, the values of ϵ_{ce} at 99% of the peak moment before and after the resisting moment has reached the peak (denoted by ϵ_{cu}' and ϵ_{cu}'' respectively) are evaluated for each beam section and the results are tabulated alongside the ϵ_{cu} values in Table 2. Since 99% of the peak moment is virtually the same as the peak moment, both ϵ_{cu}' and ϵ_{cu}'' may be regarded as alternative measures of ultimate concrete strain. Any value between ϵ_{cu}' and ϵ_{cu}'' may be chosen as the design value of ultimate concrete strain.

In order to be applicable throughout the ranges of compression and tension steel ratios covered in this study, the design value of ultimate concrete strain for the given concrete grade should be greater than the maximum value of ϵ_{cu}' and smaller than the minimum value of ϵ_{cu}'' within the entire ranges of compression and tension steel ratios considered. In all cases, including the particular case of $f_{co} = 60$ MPa presented in Table 2, the minimum value of ϵ_{cu}'' is found to be slightly larger than the maximum value of ϵ_{cu}' . Thus, the mean of the maximum value of ϵ_{cu}' and the minimum value of ϵ_{cu}'' is taken as the design value of ultimate concrete strain for the given concrete grade. The design values of ultimate concrete strain so evaluated for each concrete grade are presented in Table 3. By curve fitting, the following equation for evaluating the design value of ultimate concrete strain is obtained:

Table 3 Recommended design values of ultimate concrete strain (in $\mu\epsilon$)

f_{co} (MPa)	Design value of ϵ_{cu} derived from ϵ_{cu}' and ϵ_{cu}''	Design value of ϵ_{cu} derived from Eq. (12)
30	3225	3195
40	3175	3170
50	3130	3145
60	3095	3120
70	3070	3095
80	3055	3070
90	3045	3045
100	3040	3020

$$\epsilon_{cu} = 3270 - 2.5 f_{co} \tag{12}$$

in which ϵ_{cu} is in micro-strain and f_{co} in MPa. The design value of ϵ_{cu} evaluated by this equation is accurate to within 30 micro-strain for f_{co} ranging from 30 to 100 MPa, as depicted in Table 3. In fact, the ϵ_{cu} value of a given concrete grade so derived is always within the range between the maximum value of ϵ_{cu}' and the minimum value of ϵ_{cu}'' of the concrete grade and therefore the use of this equation would produce less than 1% error in the calculated value of flexural strength.

7. Ductility analysis

The flexural ductility is measured in terms of a ductility factor μ given by:

$$\mu = \phi_u / \phi_y \tag{13}$$

where ϕ_u and ϕ_y are the ultimate curvature and yield curvature respectively. The ultimate curvature ϕ_u is taken as the curvature at which the resisting moment has, after reaching the peak, dropped to

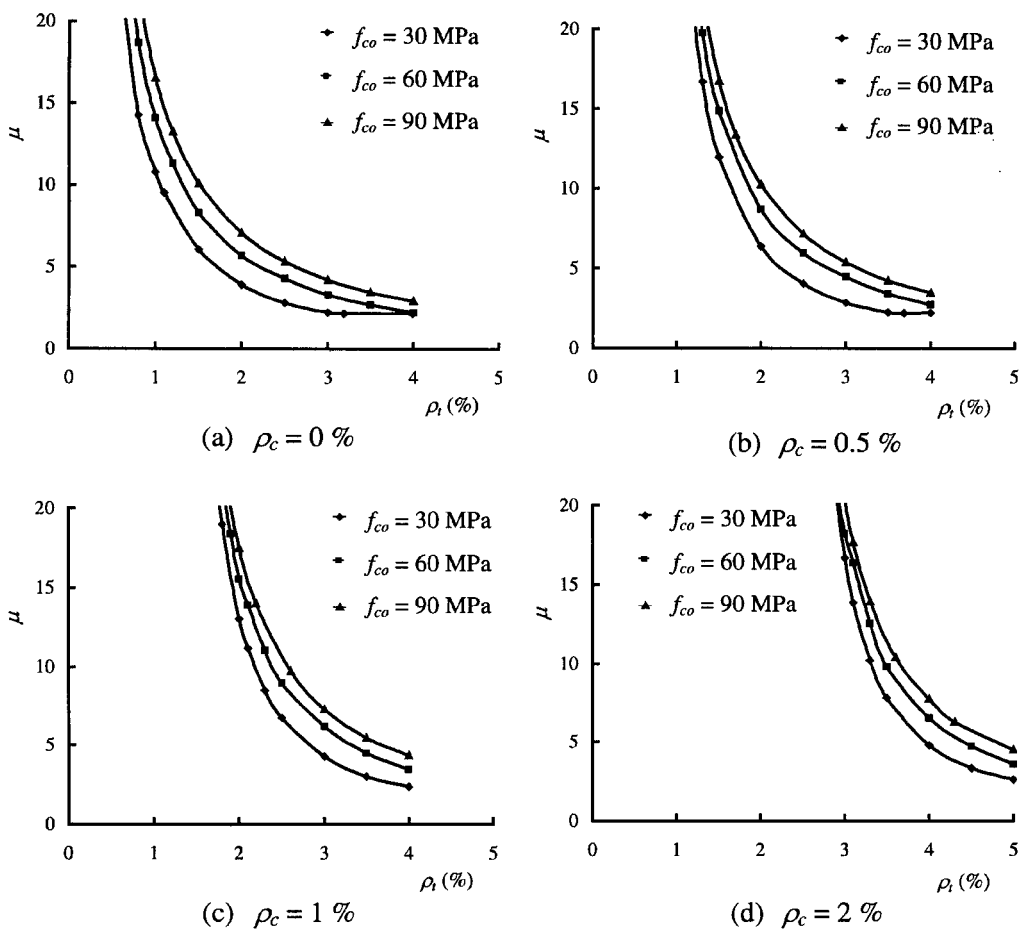


Fig. 6 Ductility factor plotted against tension steel ratio ρ_t

80% of the peak moment. On the other hand, the yield curvature ϕ_y is defined as the curvature at the hypothetical yield point of an equivalent elasto-plastic system whose equivalent elastic stiffness is taken as the secant stiffness at 75% of the peak moment before the peak moment is reached and yield strength is taken as the peak moment; the yield curvature so defined is actually equal to the curvature at 75% of the peak moment divided by 0.75.

The values of μ so evaluated are plotted against the corresponding values of tension steel ratio ρ_t in Fig. 6. It is seen that at a given concrete grade and a given compression steel ratio, the ductility factor decreases as the tension steel ratio increases. On the other hand, at a given concrete grade and a given tension steel ratio, the ductility factor increases as the compression steel ratio increases. However, the effect of the concrete grade on the ductility factor is more complicated. At given compression and tension steel ratios, the ductility factor seems to increase slightly with the concrete grade albeit a higher grade concrete should be less ductile. This is because the major factor affecting the flexural ductility is actually the degree of the beam section being under-reinforced or over-reinforced. As the concrete grade increases, the balanced steel ratio ρ_b also increases and consequently the tension steel to balanced steel ratio (ρ_t/ρ_b) is reduced leading to an increase in the degree of being under-reinforced or a decrease in the degree of being over-reinforced. The increase in flexural ductility due to the reduction in the (ρ_t/ρ_b) ratio has out-weighed the decrease in flexural

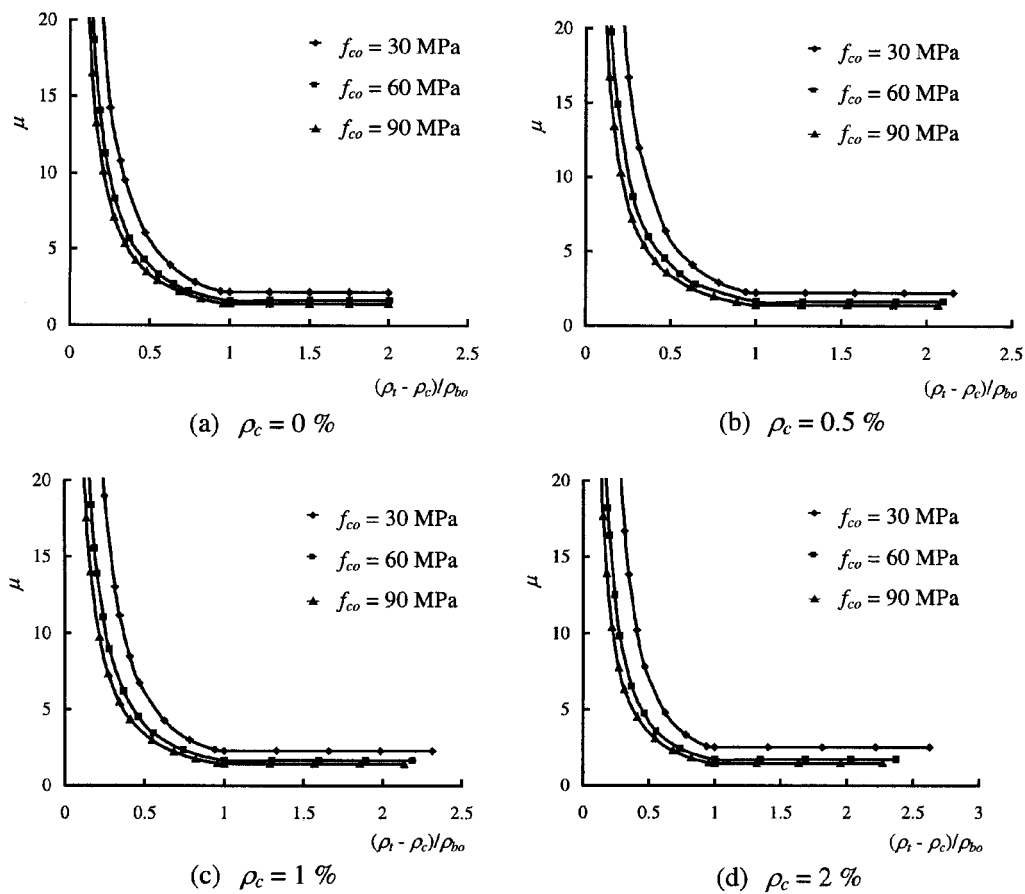


Fig. 7 Ductility factor plotted against the $(\rho_t - \rho_c)/\rho_{bo}$ ratio

ductility due to the reduction in ductility of the concrete.

For doubly reinforced sections, however, there are two different ways of measuring the degree of the section being under- or over-reinforced, one in terms of the ratio $(\rho_t - \rho_c)/(\rho_{bo})$ and the other in terms of the ratio $(\rho_t)/(\rho_{bo} + \rho_c)$. Both these two ratios are smaller than 1.0 for under-reinforced sections, equal to 1.0 for balanced sections, and larger than 1.0 for over-reinforced sections. To study how these two ratios affect the flexural ductility, μ is plotted against $(\rho_t - \rho_c)/(\rho_{bo})$ in Fig. 7 and against $(\rho_t)/(\rho_{bo} + \rho_c)$ in Fig. 8. It can now be seen that at a given $(\rho_t - \rho_c)/(\rho_{bo})$ or $(\rho_t)/(\rho_{bo} + \rho_c)$ ratio, the flexural ductility decreases as the concrete grade increases.

In a previous study by the authors (Ho *et al.* 2001) on the flexural ductility of singly reinforced sections, the relationship between μ and the parameters f_{co} and ρ_t for sections with no compression reinforcement provided has been derived as:

$$\mu = 10.7 (f_{co})^{-0.45} (\rho_t/\rho_{bo})^{-1.25} \tag{14}$$

in which ρ_t should be taken as equal to ρ_b when ρ_t is greater than ρ_b (μ is independent of ρ_t when ρ_t is greater than ρ_b). This formula produces less than $\pm 10\%$ error in μ within the same range of structural parameters covered in this study. It is proposed to extend this formula for application to

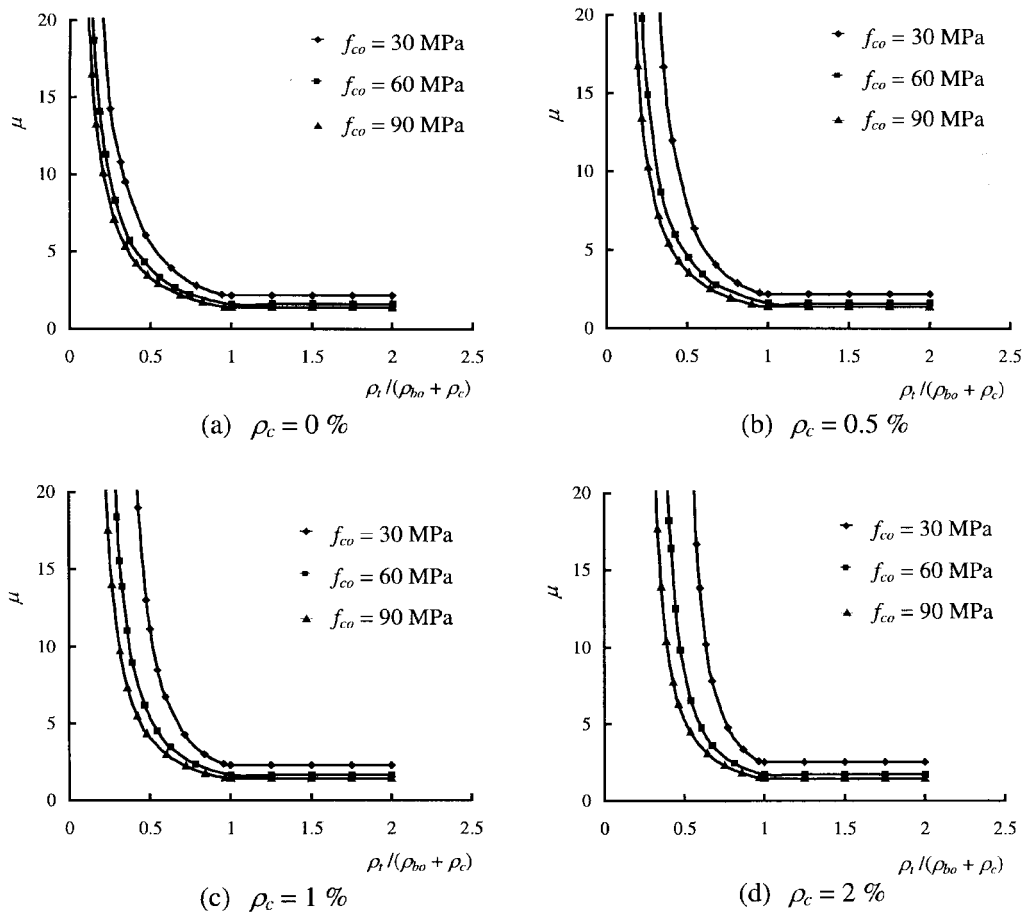


Fig. 8 Ductility factor plotted against the $\rho_t/(\rho_{bo} + \rho_c)$ ratio

doubly reinforced sections by adding an extra term to the formula to allow for the effect of providing compression reinforcement. However, before doing so, the term (ρ_t/ρ_{bo}) , which serves as a measure of the degree of the section being under- or over-reinforced in singly reinforced sections, needs to be replaced by either $(\rho_t - \rho_c)/(\rho_{bo})$ or $(\rho_t)/(\rho_{bo} + \rho_c)$. Hence, there are two ways of extending these formulas. Replacing (ρ_t/ρ_{bo}) by $(\rho_t - \rho_c)/(\rho_{bo})$ and adding an extra term $f_1(\rho_c)$, the following formula is obtained:

$$\mu = 10.7 (f_{co})^{-0.45} ((\rho_t - \rho_c)/\rho_{bo})^{-1.25} f_1(\rho_c) \quad (15)$$

On the other hand, replacing (ρ_t/ρ_{bo}) by $(\rho_t)/(\rho_{bo} + \rho_c)$ and adding an extra term $f_2(\rho_c)$, the following formula is obtained:

$$\mu = 10.7 (f_{co})^{-0.45} (\rho_t/(\rho_{bo} + \rho_c))^{-1.25} f_2(\rho_c) \quad (16)$$

The numerical values of the extra term $f_1(\rho_c)$ have been determined by solving Eq. (15) using the given values of f_{co} , ρ_t and ρ_c and the corresponding theoretical values of μ evaluated by the nonlinear flexural analysis. Fig. 9 shows how $f_1(\rho_c)$ varies with f_{co} , ρ_t and ρ_c . Curve fitting yields the following equation:

$$f_1(\rho_c) = 1 + 95.2(f_{co})^{-1.1} (\rho_c/\rho_t)^3 \quad (17)$$

in which ρ_t should be taken as equal to ρ_b when ρ_t is greater than ρ_b . Substituting back to Eq. (15), the following formula for direct evaluation of the flexural ductility of doubly reinforced beam sections is derived:

$$\mu = 10.7 (f_{co})^{-0.45} ((\rho_t - \rho_c)/\rho_{bo})^{-1.25} (1 + 95.2(f_{co})^{-1.1} (\rho_c/\rho_t)^3) \quad (18)$$

in which, as before, ρ_t should be taken as equal to ρ_b when ρ_t is greater than ρ_b . Within the ranges of structural parameters studied, the values of μ obtained by this formula are accurate to within $\pm 10\%$ error.

The numerical values of the extra $f_2(\rho_c)$ term have also been determined in a similar way. However, no simple equation could be found for $f_2(\rho_c)$. It does not seem that Eq. (16) would yield any simple and yet accurate formula for direct evaluation of μ . This is probably because relatively speaking the ratio $(\rho_t)/(\rho_{bo} + \rho_c)$ is not as good as the ratio $(\rho_t - \rho_c)/(\rho_{bo})$ as a measure of the degree of the section being under- or over-reinforced.

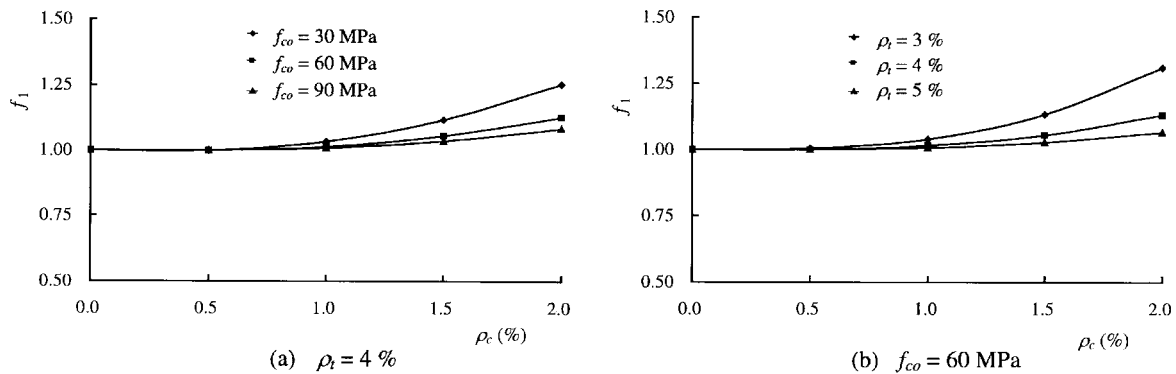


Fig. 9 The extra term $f_1(\rho_c)$ plotted against compression steel ratio ρ_c

From Eq. (18), it can be seen that the addition of compression reinforcement has two effects. Firstly, it decreases the degree of the section being over-reinforced by decreasing the ratio $(\rho_t - \rho_c)/(\rho_{bo})$. Secondly, it increases the ductility factor through the term $f_1(\rho_c)$. Although the addition of compression reinforcement is generally quite costly, it is very effective in increasing the flexural ductility. For instance, the addition of 1% compression reinforcement could increase the ductility factor by as much as 40%.

8. Conclusions

The nonlinear flexural behavior of doubly reinforced concrete beam sections have been evaluated using a newly developed analysis method that takes into account the stress-path dependence of the stress-strain relation of the tension reinforcement. By analyzing beam sections with or without compression reinforcement provided and made of concrete with in-situ compressive strength ranging from 30 to 100 MPa, a comprehensive parametric study has been carried out. From the study, the following conclusions may be drawn. (1) Strain reversal of the tension reinforcement occurs in both singly and doubly reinforced sections. (2) The balanced steel ratio of a doubly reinforced section increases linearly with the compression steel ratio. (3) The ultimate concrete strain varies with the compression and tension steel ratios in a fairly complicated manner but for practical applications, the design values of ultimate concrete strain derived herein, which are independent of the steel ratios, may be used. (4) The flexural ductility decreases with the tension steel ratio but increases with the compression steel ratio. At given steel ratios, the flexural ductility increases with the concrete grade but at a given degree of the section being under- or over-reinforced, the flexural ductility decreases as the concrete grade increases.

Finally, by correlating the ductility factors of the beam sections to the structural parameters involved, a formula for direct evaluation of the flexural ductility of doubly reinforced normal- and high-strength concrete beam sections has been developed. Within the ranges of structural parameters studied, this formula is accurate to within $\pm 10\%$ error. It reveals the possible effects of adding compression reinforcement on flexural ductility and may be used to develop guidelines for the ductility design of doubly reinforced high-strength concrete beam sections.

Acknowledgement

The work described herein was carried out with financial support provided by the Research Grants Council of Hong Kong (RGC Project No. HKU 7012/98E).

References

- ACI Committee 363 (1992), "State-of-the-art report on high strength concrete", ACI 363-R92, American Concrete Institute, Detroit, U.S.A., 55pp.
- Attard, M.M., and Setunge, S. (1996), "The stress strain relationship of confined and unconfined concrete", *ACI Mater. J.*, **93**(5), 432-442.
- Attard, M.M., and Stewart, M.G. (1998), "A two parameter stress block for high-strength concrete", *ACI Struct.*

- J.*, **95**(3), 305-317.
- Carreira, D.J., and Chu, K.H. (1986), "The moment-curvature relationship of reinforced concrete members", *ACI J.*, **83**(2), 191-198.
- Ho, J.C.M., Pam, H.J., and Kwan, A.K.H. (2001), "Theoretical analysis of complete moment-curvature behavior of reinforced high-strength concrete beams", *Eng. Struct.* (to be published).
- Pam, H.J., Kwan, A.K.H., and Islam, M.S. (2001), "Flexural strength and ductility of reinforced normal- and high-strength concrete beams", *Proc., Institution of Civil Engineers, Structures and Buildings* (to be published).
- Park, R., and Paulay, T. (1975), *Reinforced Concrete Structures*, John Wiley & Sons, New York, U.S.A., 769pp.
- Samra, R.M., Deeb, N.A.A., and Madi, U.R. (1996), "Transverse steel content in spiral concrete columns subjected to eccentric loading", *ACI Struct. J.*, **93**(4), 412-419.
- Sheikh, S.A., and Yeh, C.C. (1997), "Analytical moment-curvature relations for tied concrete columns", *J. Struct. Eng.*, ASCE, **118**(2), 529-544.

Notation

- A_{sc}, A_{st} : areas of compression and tension reinforcement
 b, d : breadth and effective depth of beam section
 d_f : depth of compression reinforcement
 d_n : neutral axis depth
 E_c, E_s : Young's moduli of concrete and steel reinforcement
 f_c : cylinder compressive strength of concrete
 f_{ci} : stress at inflection point on descending branch of stress-strain curve
 f_{co} : in-situ uniaxial compressive strength of concrete
 f_y : yield strength of steel reinforcement
 h : total depth of beam section
 M : resisting moment of beam section
 P : applied axial load to beam section
 x : distance from neutral axis
 $\epsilon_c, \epsilon_{ce}$: strain in concrete and strain in concrete at extreme compression fiber
 ϵ_{co} : strain in concrete at peak stress
 ϵ_{ci} : strain at inflection point on descending branch of stress-strain curve
 ϵ_{cu} : ultimate concrete strain (value of ϵ_{ce} at peak moment)
 ϵ_p : residual plastic strain in steel reinforcement
 ϵ_s : strain in steel reinforcement
 $\epsilon_{sc}, \epsilon_{st}$: strains in compression and tension reinforcement
 ϵ_y : yield strain of steel reinforcement
 ϕ : curvature of beam section
 ϕ_u, ϕ_y : ultimate and yield curvatures of beam section
 μ : ductility factor
 ρ_b : balanced steel ratio of beam section
 ρ_{bo} : balanced steel ratio of beam section with no compression steel
 ρ_c, ρ_t : compression steel ratio ($\rho_c = A_{sc}/bd$) and tension steel ratio ($\rho_t = A_{st}/bd$)
 σ_c, σ_s : stresses in concrete and steel reinforcement
 σ_{sc}, σ_{st} : stresses in compression and tension reinforcement